Romanian Reports in Physics, Vol. 62, No. 3, P. 581–593, 2010

Dedicated to the 50th LASER Anniversary
(LASERFEST-50)

NON-LINEAR RAMAN SCATTERING EFFECTS GENERATED BY THE SURFACE PLASMONS EXCITATION

I. BALTOG, M. BAIBARAC, L. MIHUT, I. SMARANDA

National Institute of Material Physics, Atomistilor 105 bis. P.O.Box MG-7,
RO-077125 Bucharest-Magurele, Romania,
E-mail: ibaltog@infim.ro

(Received May 31, 2010)

Abstract. An inciting and much debated subject in the surface enhanced Raman (SERS) studies is an unusual anti-Stokes Raman spectrum distinguished by an abnormal intensity, increasing with the vibrational wavenumber and some discrepancies with regard to the Stokes spectrum. We demonstrate that the abnormal anti-Stokes Raman emission on single walled carbon nanotubes and poly(3,4-ethylenedioxy thiophene) synthtetized electrochemically appears as a consequence of two corroborating effects: resonance, which occurs when the energy of the excitation light is near or coincident with the energy of an electronically allowed transition, and the SERS effect achieved by the excitation of surface plasmons. An abnormal intense Raman emission in the Stokes branch, reminiscent to a stimulated Raman effect, which increases exponentially with the intensity of exciting light is reported for the first time in the case of SWNTs.

Key words: plasmons, carbon nanotubes, resonant Raman scattering, surface enhanced Raman scattering.

1. INTRODUCTION

Raman spectroscopy is a widely used analytical tool capable of providing valuable information about the chemical structure and composition of molecules. Discovery of lasers, as intense monochromatic light sources, have favored an intensiv the development of researches in the field. Recently a major effort was aimed to the developing of highly sensitive experimental techniques capable of supplying new data on the molecular architecture of the nanoscaled materials and on the nature of interactions between components is of primary importance for surface analysis. One of these techniques is the surface-enhanced Raman scattering (SERS). Over time, many investigators have attempted to explain the unexpectedly

large enhancement in terms either of an electromagnetic [1] or a chemical effect [2]. It is now widely accepted that a combination of both effects are actually responsible for the SERS phenomenon [3]. However, the electromagnetic mechanism seems to be the most important in SERS generation, it consists in the excitation of localized and delocalized surface plasmons (SPs) [4]. The delocalized surface plasmons are surface evanescent waves that propagate along the interface between the metal and the surrounding dielectric medium. A *p*-polarized incident beam can be coupled to these surface waves through an optical coupler, which can be a prism or a diffraction grating under certain angle of incidence [5]. The intense electromagnetic field that exists at the interface between the metal and the surrounding medium excites Raman transitions in the molecules adsorbed on the metal surface. Depending on the optical coupler, part of the Raman radiation thus produced excites in turn surface plasmons at the Stokes frequency, and then decouples as a propagating Raman radiation in the interior of the prism [6] or as diffracted light in a well-defined direction dependent on the grating periodicity [7]. For current SERS studies, the use of the prisms or gratings as optical couplers is rather cumbersome. An efficient method is to use a rough metal support. Qualitatively, the rough metal support may be considered a superposition of diffraction gratings with different periods, each period being smaller than the wavelength of the exciting radiation. In this case, the morphology of the metal surface becomes very important for SERS spectroscopy. The strong dependence of the SERS spectrum intensity on metal support roughness [1-3] imposes certain restrictions on the technique of preparation of the metal films. Reproducible results were reported using as SERS support a metallic film prepared by the vacuum evaporation technique with the atomic beam at almost grazing incidence ($\theta \approx 80^{o}$) on the microscope slide used as a target support [8]. A typical aspect of a rough gold surface with a good Raman activity is presented in Fig.1. For such a surface having a columnar structure of mean diameter much smaller than the wavelength of the exciting radiation, the enhanced fields, consisting of evanescent components, are strongly confined to the tip end. As result of the intense concentration of electromagnetic field via the excitation of localized surface plasmons various linear and non-linear optical phenomena may be generated in the molecules from proximity.

The chemical contribution to the SERS process is more difficult to identify or assess in quantitative terms. The chemical mechanism contributing to Raman scattering exaltations is based on an increased polarizability of the molecules adsorbed on rough metallic surface under the influence of incident radiation.

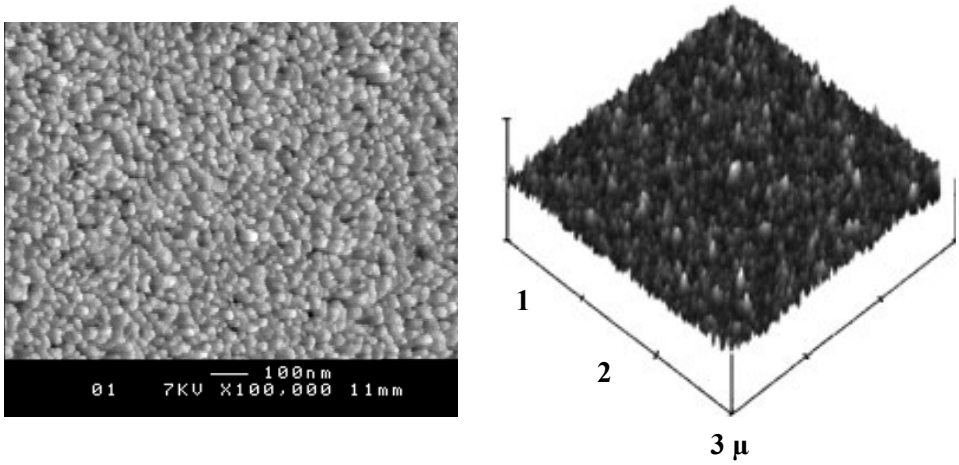

Fig. 1 – FSEM (left) and AFM (right) pictures of rough Au support.

Due to the new chemical bonds formed via a charge transfer from metal to adsorbed molecules, the polarizability of adsorbed molecules becomes much higher than that of free molecules [9]. Such a process may be considered similar to resonant Raman scattering that occurs when the energy of the excitation light coincides with the energy of electronic transitions, when new terms associated with the dielectric susceptibility appear in the polarizability expression. These terms are of higher order*, i.e.,* second, $\chi^{(2)}$, third $\chi^{(3)}$, which becoming different from zero fulfill the main requirement for generating non-linear optical processes.

From all above one may conclude that in the case of a SERS measuring configuration two effects may contribute to rise of a non linear optical process, one relates the resonant electronic excitation, when $\chi^{(2)}$, $\chi^{(3)}$ become different from zero and another the electromagnetic field confination at the metal/dielectric interface.

In what follows we demonstrate the producing of two optical phenomena, reminiscent to a non-linear optical processes: i) an anomaly anti-Stokes emission, reminiscent of a non-linear optical process of Coherent anti-Stokes Raman Scattering (CARS) type, which appears when the energy of the exciting light is close to or coincident with the energy of an electronically allowed transition ii) a Stokes Raman emission increasing non-linearly with the intensity of excitation light that is generated by a SERS mechanism when a diffraction grating is used as optical coupler. For this we use as demonstrating material poly(3,4-ethylenedioxy thiophene) (PEDOT) and single walled carbon nanotubes (SWNTs) under two excitation wavelengts , 676.4 and 514.5 nm , both ensuring a rezonant excitation of PEDOT and metallic SWNTs.

2. EXPERIMENTAL

SERS experiments were performed at excitation light of 676.4 and 514.5 nm using a Krypton and Argon laser, respectively. Two types of SERS supports were used: i) Au films with a mean roughness of about 30-100 nm, which were obtained by the vacuum evaporation with a deposition rate of ca. 1 nm/sec at a pressure $< 10^{-5}$ torr with the atomic beam at constant grazing incidence ($\beta_{in} \sim 85^{o}$) on the microscope slide used as target; ii) a ruled diffraction grating, with sinusoidal groove profile and periodicity $d = 833$ nm, covered with Au. SWNTs films were obtained by evaporating a solvent (toluene) from a uniformly distributed emulsion of nanotubes spread on Au substrates.

The electrochemical polymerization of monomer 3,4-ethylene dioxythiophene (EDOT) was performed in a conventional three-electrode one-compartment cell having as working electrode an Au support or a SWNT film deposited on a 1 cm^2 Au plate. The auxiliary electrode was a spiral Pt wire. The potential of the working electrode was measured vs. an Ag/AgCl electrode. The solutions of 0.05 M EDOT and 0.1 M $LiClO_4$ in CH_3CN were argon purged prior to recording the cyclic voltammograms. Poly(3,4-ethylenedioxy thiophene) (PEDOT) was electrochemically synthesized by cyclic voltammetry (CV) in the potential range of (–1000; +1600) mV vs. Ag/Ag^+ and a sweep rate of 100 mV s^{-1} both on a blank Au electrode and an Au electrode covered with a SWNT film. The electrochemical measurements were carried out using a potentiostat/galvanostat VOLTALAB 80 model, from Radiometer Analytical.

SERS spectra were recorded at room temperature in air, in a backscattering geometry, using a Jobin Yvon T64000 Raman-spectrophotometer endowed with a microprobe allowing the laser light to be focused to a dot on the sample with a micrometer accuracy. The Stokes and anti-Stokes Raman emission is collected as ±1 diffracted order by a microscope objective with a suitable numerical aperture.

3. RESULTS AND DISCUSSION

Figure 2a illustrates a suitable configuration of measuring of the Raman emission excited by surface plasmons when a diffraction grating is used as optical coupler. Figures 2b show the impact spots of exciting radiation on two types of SERS supports: i) a gold film with the average roughness of 30-10 nm and ii) a diffraction grating covered with Au film that does not alter the grating profile characteristics. In the latter case is important to note the formation of surface plasmons that propagate perpendicularly to the grooves direction. Raman emission emerging as diffracted light of 1st order is collected by a microscope objective of suitable aperture.

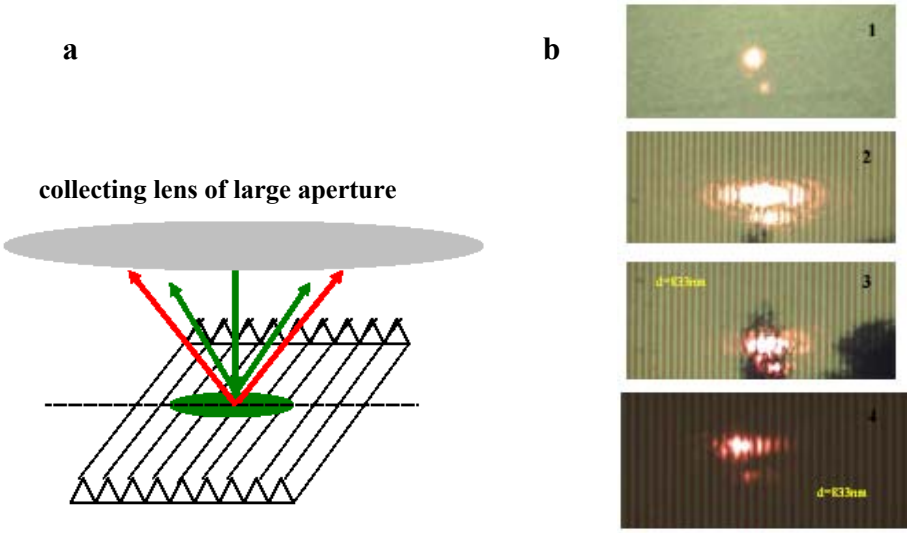

Fig. 2 – Propagative plasmon excitation on diffraction grating. Impact spots of exciting radiation on gold film with the average roughness of 30-10 nm (1), diffraction grating alone (2) and covered with carbon nanotubes (3) and CuPc films (4).

Normally, the spontaneous Raman emission is characterized by weak signals (~10^{-6} in comparison with the intensity of exciting light) forming the two Stokes and anti-Stokes branches, which have the relative intensities established by the Maxwell-Boltzmann formula, Eq.1, that describes the distribution of population in the involved vibrational states.

$$\frac{I_{anti-Stokes}}{I_{Stokes}} = \left(\frac{\sigma(\alpha_\Omega)_{anti-Stokes}}{\sigma(\alpha_\Omega)_{Stokes}} \right) \left(\frac{\omega_0 + \Omega}{\omega_0 - \Omega} \right)^4 \exp\left(\frac{h\Omega}{kT} \right)^{-1}. \quad (1)$$

In equation (1), ω_0 and Ω , h , k and T are the wavenumbers of excitation light and Raman line (cm^{-1}), and h , k and T are the Planck constant, the Boltzmann constant and temperature, respectively. Illustratively, in the Eq.1 the terms $\sigma(\alpha_\Omega)_{anti\text{-}Stokes}$ and $\sigma(\alpha_\Omega)_{Stokes}$ indicate the anti-Stokes and Stokes cross sections associated to the Ω wavenumber. These terms dependent on the polarizability of material, they being equal for normal (non-resonant) spontaneous Raman process. Raman spectrum excited by surface plasmons reveals as fundamental characteristics an enhancement of the Stokes branch and an anomaly anti-Stokes emission which increases in intensity when the energy of the exciting light is close to or coincident with the energy of an electronically allowed transition. The latter process being named also resonant Raman scattering (RRS)[10].

Raman light scattering is an example of a complex interaction between the incident electromagnetic wave (*EM*) and the material's molecular/atomic structure.

Under the oscillating *EM* field of the exciting light a periodic separation of charge results in the electron cloud which is called an induced molecular dipole moment, *P*. The oscillating induced dipole moment manifests itself as a source of secondary *EM* radiation, thereby resulting in scattered light. The strength of the induced dipole moment, $\boldsymbol{P}$, is given by $\boldsymbol{P} = \alpha \boldsymbol{E}$, where α is the polarizability and $\boldsymbol{E} = \boldsymbol{E}_0(\cos 2\omega_0 t + \varphi_0)$ is the strength of electric field of the incident EM wave. On the macroscopic scale, the response of a material to resonant EM excitation is described by polarization $\boldsymbol{P} = \boldsymbol{P_0} + \chi^{(1)} \boldsymbol{E} + \chi^{(2)} \boldsymbol{EE} + \chi^{(3)} \boldsymbol{EEE} + \ldots$ followed by higher order terms. The use of SERS supports, suitable for the surface plasmons excitation, determines a strong confination of the electromagnetic field at the metal/dielectric interface. Thus, the terms of higher order as $\chi^{(2)} \boldsymbol{EE}$ and $\chi^{(3)} \boldsymbol{EEE}$ that appears in the polarization expression amount to fulfilling the key condition to generate a nonlinear optical process [33], they summarize the contribution of two effects, one related to the resonant electronic excitation, when $\chi^{(2)}$, $\chi^{(3)}$ become different from zero and another to the electromagnetic field confination at the metal/dielectric interface.

The literature of recent years reveals an increased interest for the Raman studies in Stokes and anti-Stokes branches and in this context, carbon nanotubes were among the most studied materials [11–17].

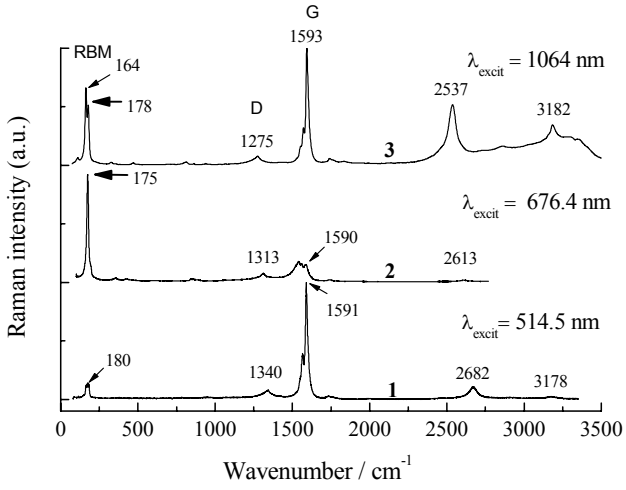

Fig. 3 – SERS spectra, at $\lambda_{exc.}$ = 514.5 nm (1), 676.4 nm (2) and = 1064 nm (3) of carbon nanotube films of ca. 150 nm thickness deposited on rough Au supports.

Figure 3 reminds the reader that the Raman spectra of SWNTs exhibits three main groups of bands whose relative intensities and peak positions vary with excitation wavelength. In the first group, at low wavenumbers, one finds the bands associated with radial breathing vibration modes (RBM), whose peak positions are related to the tube diameter (*d*). At resonant excitation these bands appear strongly

enhanced, i.e. at λ_{exc} = 1 064 nm semiconducting tubes and λ_{exc} = 676.4 nm metallic tubes. The second group, consisting of G and D bands, which are not only related to the nanotube structure, covers the interval from 1000 to 1700 cm^{-1}.The former, peaking at about 1,595 cm^{-1} is attributed to the tangential vibration mode (TM) and the latter, the D band, whose peak position varies with the excitation wavelength is often associated with a disorder or defect states induced in the graphitic lattices or nanotubes. A third group, ranging between 2 500 and 3 500 cm^{-1}, contains Raman lines of second order [18].

Returning to the anti-Stokes Raman spectra of SWNTs, the high values of the anti-Stokes/Stokes intensity ratio (I_{aS}/I_S) and the different line shapes of the G band at about 1595 cm^{-1} could be considered as distinguishing features of a nonlinear optical process. Such an abnormal anti-Stokes emission is presented in Fig. 4. If the strength effect is measured by the ratio value $\rho = \left(\frac{I_{aS}^{\exp}}{I_{aS}^{calc}} \right)_{\Omega}$, one observes that it becomes unity for non-resonance, when the process is governed by a Boltzmann distribution of populations in the excited vibrational states. I_{aS}^{calc} is the anti-Stokes Raman replica calculated with the formula (1) applied to the Stokes Raman spectrum. Referring to the G band of SWNTs and for the same thickness, we found ρ = 4.34 and 125 at $\lambda_{exc.}$ = 514.5 and 676.4, nm respectively. The more intense anti-Stokes Raman emission observed at $\lambda_{exc.}$ = 676.4 nm in comparison with λ_{exc} = 514.5 nm must be correlated with the strong resonant electronic excitation of metallic nanotubes, condition fulfilled in the former case. SWNTs with a diameter around 1.35 nm exhibit in the UV-VIS-NIR spectrum three mean absorption bands peaking at about 0.68 eV (1823 nm), 1.2 eV (1033 nm) and 1.68 eV (738 nm) attributed to the interband transitions between the E_{11}^{S}, E_{22}^{S} and E_{11}^{M} van Hove density of states singularities. The first two bands have been assigned to gap transitions in semi-conducting tubes, while the third one originates from metallic tubes [18].

Scrupulous investigations performed at resonant optical excitation have revealed new dependences for the anti-Stokes emission: i) the intensity of anti-Stokes Raman lines increases with the vibrational wavenumber; ii) a square dependence on the film thickness; iii) a square dependence on the exciting laser intensity; iv) a linear dependence on the numerical aperture *(NA)* of the microscope objective used for the detection of the anti-Stokes emission ; v) the polarization ratio on the anti-Stokes side is always greater in comparison with that measured for a spontaneous Stokes Raman emission. All these features cannot be explained by existing theories associated with a resonant Raman effect and surprisingly, they are also encountered in the CARS type emission [16]. As a first step to finding an explanation for this abnormal anti-Stokes emission, it must to remember that, under

resonant optical excitation, when the energy of the excitation light coincides with the energy of electronic transitions, new terms associated with the dielectric susceptibility appear in the polarizability expression. These terms are of higher order, *i.e.*, second, $\chi^{(2)}$, third $\chi^{(3)}$ which becoming different from zero fulfill the main requirement for generating non-linear optical processes.

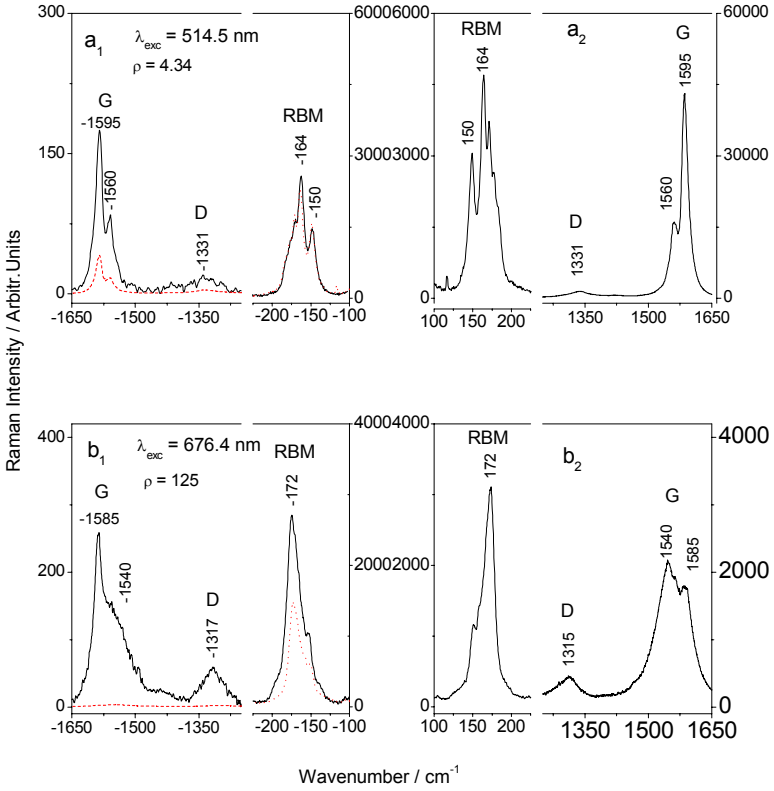

Fig. 4 – Anti-Stokes and Stokes SERS spectra, at $\lambda_{exc.}$ = 514.5 nm (a) and 676.4 nm of carbon nanotube films of ca. 150 nm thickness deposited on rough Au supports. Red (dashed) curves show the anti-Stokes replica for a non-resonant Raman effect, which is calculated with the Maxwell-Boltzmann formula applied to the Stokes spectra.

We remind the reader that CARS is a four-wave mixing process in which the anti-Stokes light (ω_{as}) results from the parametric coupling of the incident laser light (ω_l), the Stokes light (ω_s; $\omega_s < \omega_l$) and a probe light (ω_p). If $\omega_l = \omega_p$, the CARS experiment appears as a degenerate four-wave mixing process that reduces to an energy transfer between the two pump waves, ω_l and ω_s. In general, the two exciting wavelengths ω_l and ω_s, are supplied by two independent lasers or are generated by parametric wavenumber conversion. In our case, when the

investigated material is layered as a thin film on a metallic support (Au, Ag) in which surface plasmons can be excited, the second pump light ω_s, discretely distributed over all Raman transitions, may be supplied by the surface enhanced Raman scattering (SERS) mechanism. In these conditions, abnormal enhanced anti-Stokes Raman spectra having the characteristics of a CARS emission were observed on different materials under tight focusing of a single laser excitation beam. In the plane-wave approximation, the CARS intensity is described by the equation

$$I_{CARS} \propto N_A \omega_{aS}^2 d^2 \left|\chi^{(3)}\right|^2 I_l^2 I_S \sin c^2 \left(\left|\Delta k\right| d/2\right). \tag{2}$$

It reveals a particular dependence of the anti-Stokes Raman intensity on the anti-Stokes Raman shift ω_{as}, the sample slab thickness d , the incident pump intensity I_l, and the third order nonlinear dielectric susceptibility $\chi^{(3)}$. N_A is the numerical aperture of the collecting lens and sinc means $\sin(x)/x$. The coherent nature of the CARS process is reflected by fulfilling the phase-matching condition $|\Delta \boldsymbol{k}|\cdot d \ll \pi$ where $\Delta \boldsymbol{k} = \boldsymbol{k}_{as} - (2\,\boldsymbol{k}_p - \boldsymbol{k}_s)$, and $\boldsymbol{k}_{as}$, $\boldsymbol{k}_s$ and $\boldsymbol{k}_p$ are the wave vectors of the anti-Stokes, Stokes and pump light, respectively [19].

For condensed media, the small dispersion of refractive index makes $\Delta k \approx 0$, even over small paths, so that the phase matching condition is fulfilled if the beams cross at an angle θ. For tightly focused beams, the requirement of phase matching relaxes, being no longer sensitive to the Raman shift and so, a CARS spectrum can be observed at an angle θ_{as} larger than the Stokes angle θ_s [20, 21].

Another evidence of abnormal anti-Stokes Raman emission is given of PEDOT electrochemically deposited on Au rough support. The un-doped PEDOT shows an enhancement of anti-Stokes Raman spectrum (Fig. 5a) while the anti-Stokes spectrum of doped PEDOT practically coincides with the calculated spectrum with eq.1 applied to the Stokes recorded spectrum, Fig. 5b. The results can be explained from the resonant and non resonant nature of the optical excitation: PEDOT deposited by cyclic voltammetry with stopping at –1 V *vs*. Ag/Ag^+ has an un-doped form and is absorbent at 514.5 nm, while PEDOT obtained at +1.6 V *vs*. Ag/Ag^+ has a doped form, which is no longer absorbent at 514.5nm [22].

The situation is different at $\lambda_{exc.}$ = 676.4 nm (Fig. 6), when an abnormal anti-Stokes Raman effect is observed in each case due to the fact that both forms of PEDOT are absorbent. The higher electronic absorbance of PEDOT at $\lambda_{exc.}$ = 676.4 nm in the un-doped state explains the stronger anti-Stokes Raman emission (Fig. 6a) in comparison with the PEDOT in the doped state (Fig. 6b).

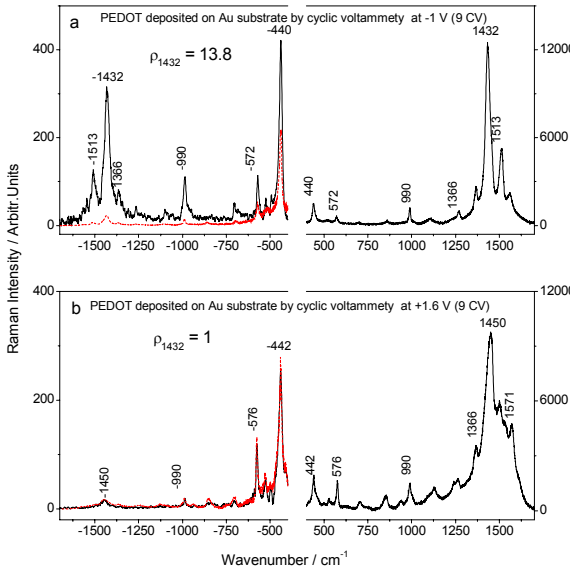

Fig. 5 – Stokes and anti-Stokes Raman spectra of PEDOT electrochemically synthesized by cyclic voltammetry with stopping at a potential of –1 V vs. Ag/Ag^+ (9 CV) (a – un-doped form) and +1.6 V vs. Ag/Ag^+ (9CV) (b – doped form) on a Au rough plate. The red (dashed) curves show the anti-Stokes replica for a non-resonant Raman effect, which is calculated with the Maxwell-Boltzmann formula applied to the Stokes spectra. λ_{exc} = 514.5 nm.

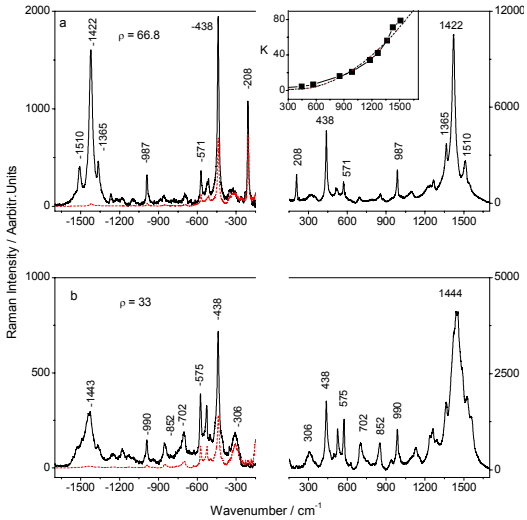

Fig. 6 – Stokes and anti-Stokes Raman spectra at resonant excitation (λ_{exc} = 676.4 nm) of PEDOT electrodeposited by cyclic voltammetry (9CV with stopping at a potential of –1 V (a) and +1.6V (b) *vs.* Ag/Ag^+) on an Au plate. The red (dashed) curves show the anti-Stokes replica for a non-resonant Raman effect, which is calculated with the Maxwell-Boltzmann formula applied to the Stokes spectra. In the inset, the experimental $K(\Omega)$ values (see text) as a function of the wavenumber are presented.

The inset of Fig. 6 reveals an important feature of the anti-Stokes Raman emission generated at a resonant optical excitation when a SERS measuring configuration is used. As in Ref.12, plotting the $K(\Omega_m)$ which is the anti-Stokes/Stokes ratio of PEDOT at various Ω_m, bands divided by the same ratio of the expected equilibrium value leads to a curve that indicates a nonlinear increase of the anti-Stokes Raman lines intensity with the vibration wavenumber. Such behavior can be related to a non-linear optical process, in agreement with Eq. 2.

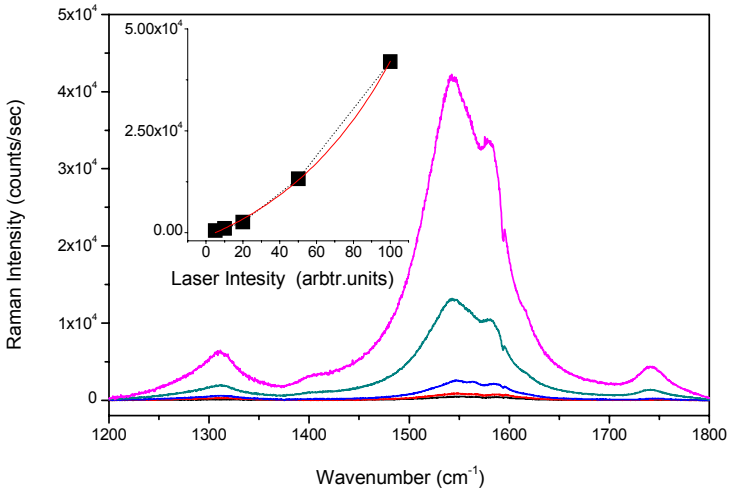

Fig. 7 – Stokes SERS spectra at resonant excitation λ_{exc} = 676.4 nm of SWNTs deposited as thin film on a diffraction grating covered with Au. In the inset reveals an exponential dependence on the intensity of the exciting light.

Let us return now to SERS measurements on carbon nanotubes deposited on a diffraction grating under resonant excitation, *i.e.* λ_{exc} = 676.4 nm. In this case one observe a non-linear increase of the Raman signal with the increase of the excitation light intensity. This fact is illustrated by Fig. 7. In agreement with the theory, the inset reveals an exponential dependence on the intensity of the exciting light. It should be noted that such dependence has been demonstrated in previous work on copper phtalocyanine (CuPc) [23].

4. CONCLUSIONS

This work demonstrates that by the surface plasmons excitation some non-linear Raman scattering effects may be generated in thin films deposited on Au support. The surface plasmons excitation has been achieved using as optical couplers both an Au films with a mean roughness of about 30-100 nm and a ruled diffraction grating, with sinusoidal groove profile and periodicity d = 833 nm,

covered with Au. An abnormal anti-Stokes Raman emission appears as consequence of two corroborating effects: i) of resonance, which occurs when the energy of the excitation light is near or coincident with the energy of an electronically allowed transition and ii) a SERS effect produced by the surface plasmons excitation. The surface plasmons excitation amounts to a strong confinement of electromagnetic field associated to exciting light. The surface plasmons excitation was obtained using two type of optical couplers: i) a Au film with a mean roughness of about 30–100 nm obtained by the vacuum evaporation at constant grazing incidence, and ii) a diffraction grating with with sinusoidal groove profile and periodicity $d = 833$ nm, covered with Au. The appearance of an abnormal anti-Stokes Raman emission was demonstrated both on single walled carbon nanotubes and poly(3,4-ethylenedioxy thiophene) synthtetized electrochemically on an Au plate. An abnormal intense Raman emission in the Stokes branch, reminiscent of a stimulated Raman effect, which increases exponentially with the intensity of exciting light is reported for the first time in the case of SWNTs.

Acknowledgments. This was supported by CNCSIS-UEFISCU, project number IDEI-No. 39/2007.

REFERENCES

1. A. Otto, *Surface Enhanced Raman Scattering*; Topics in Applied Physics, Light Scattering in Solids IV, R.K.CHANG & T.E.FURTAK, Vol. 54, Spinger Verlag, Berlin, 1984.
2. M.. Moskovits, *Surface-enhanced spectroscopy*; Rev. Modern. Phys., **57**, 783–826 (1985).
3. T.E. Furtak, *Advance in Laser Spectroscopy*, Eds.B. A. Garetz and J. R. Lombardi, Vol. **2**, Wiley, p. 175, New York, 1983.
4. H. Raether, *Surface Plasmons on Smooth and Rough Surfaces and Gratings*, in *Springer Tracts in Modern Physics*, Spinger Verlag, Berlin, 1988.
5. S. Lefrant, I. Baltog, M. Baibarac, *Surface-enhanced Raman scattering studies on chemically transformed carbon nanotube thin films,* J. Raman Spectroscopy, **36**, 676–698 (2005).
6. J. Giergiel, E. Reed, JC. Hemminger, S. Ushioda, *Surface plasmon polariton enhancement of Raman scattering in a Kretschmann geometry,* J. Phys. Chem., **92**, 5357–5365 (1988).
7. I. Baltog, N. Primeau, R. Reinisch, J.L. Coutaz, *Surface enhanced Raman scattering on silver grating: Optimized antennalike gain of the stokes signal of* 10^4, Appl. Phys. Lett.**, 66**, 1187–1189 (1995).
8. J.L. Martinez, Y. Gao, T. Lopez-Rios, *Surface-enhanced Raman scattering spectra of p-nitrobenzoate on obliquely evaporated Ag films are presented. A surface anisotropy of the Raman enhancement for grazing evaporation angles was found*, Phys. Rev. B, **33**, 5917–5919 (1986).
9. A. Otto, I. Mrozek, H. Grabhorh, W. Akermann, *Surface enhanced Raman scattering,* J. Condens. Matter, **4**, 1143–1212 (1992).
10. D.L. Rousseau, J.M. Friedman, P.F. Williams, in *Topics in Current Physics*, Vol. 11 (Ed.A.Weber), Springer, Berlin, 1979, pp. 203–254.
11. K. Kneipp, Y. Wang, H. Kneipp, I. Itzkan, R.R. Dasari, M.S. Feld, *Population Pumping of Excited Vibrational States by Spontaneous Surface-Enhanced Raman Scattering,* Phys.Rev.Lett., **76**, 2444–2447 (1996).
12. T.L. Haslett, L. Tay, M. Moskovits, *Can surface-enhanced Raman scattering serve as a channel for strong optical pumping?* J. Chem. Phys., **113**, 1641–1646 (2000).

13. S.D.M. Brown, P. Corio, A. Marucci, M.S. Dresselhaus, M.A. Pimenta, K. Kneipp, *Anti-Stokes Raman spectra of single-walled carbon nanotubes* Phys.Rev.B, **61**, R5137–R5140 (2000).
14. L.G. Cancado, M.A. Pimenta, R. Saito, A. Jorio, L.O. Ladeira, A. Grueneis, A.G. Souza Filho, G. Dresselhaus, M.S. Dresselhaus, *Stokes and anti-Stokes double resonance Raman scattering in two-dimensional graphite*, Phys.Rev. B, **66**, 35415 (2002).
15. A.G. Brolo, A.C. Sanderson, A.P. Smith, *Ratio of the surface-enhanced anti-Stokes scattering to the surface-enhanced Stokes-Raman scattering for molecules adsorbed on a silver electrode,* Phys.Rev.B, **69**, 045424 (2004).
16. I. Baltog, M. Baibarac, S. Lefrant, *Coherent anti-Stokes Raman scattering on single-walled carbon nanotube thin films excited through surface plasmons,* Phys. Rev. B,**72**, 245402 (2005).
17. M. Baibarac, I. Baltog, S. Lefrant, *Raman spectroscopic evidence for interfacial interactions in poly(bithiophene)/single-walled carbon nanotube composites*, Carbon, **47**, 1389–1398 (2009).
18. M.S. Dresselhaus, G. Dresselhaus, R. Saito, A. Jorio, *Raman spectroscopy of carbon nanotubes,* Physics Reports, **409**, 47–99 (2005).
19. Y.R**.** Shen, *The Principle of Nonlinear Optics*; John Wiley & Sons,Inc.,Hoboken, New Jersey, 2002, pp. 242–266.
20. M. Müller, J.M. Schins, *Imaging the Thermodynamic State of Lipid Membranes with Multiplex CARS Microscopy,* J. Phys. Chem. B, **106**, 3715–3723 (2002).
21. J.X. Cheng, A. Volkmer, L. Book, X.S. Xie, *Multiplex Coherent Anti-Stokes Raman Scattering Microspectroscopy and Study of Lipid Vesicles*, J. Phys. Chem. B**, 106**, 8493–8498 (2002).
22. S. Garreau, G. Louarn, J.P. Buisson, G. Froyer, S. Lefrant, *In Situ Spectro-Electrochemical Raman Studies of Poly(3,4-ethylenedioxythiophene) (PEDT),* Macromolecules, **32**, 6807–6812, (1999).
23. I. Baltog, N. Primeau, R. Reinisch, J.L. Coutaz, *Observation of stimulated surface-enhanced Raman scattering through grating excitation of surface plasmons,* J. Opt. Soc. Am. B, **13**, 656–660 (1996).